Available online at www.sciencedirect.com
SCIENCE DIRECT®
ELSEVIER
International Journal of Solids and Structures 42 (2005) 3059–3074
INTERNATIONAL JOURNAL OF SOLIDS and STRUCTURES
www.elsevier.com/locate/ijsolstr

Stress singularity analysis around the singular point on the stress singularity line in three-dimensional joints

Monchai Prukvilailert [a,*], Hideo Koguchi [b]

[a] *Department of Mechanical Engineering, Graduate School of Nagaoka University of Technology, Kamitomioka 1603-1, Nagaoka, Niigata, 940-2188, Japan*
[b] *Department of Mechanical Engineering, Nagaoka University of Technology, Kamitomioka 1603-1, Nagaoka, Niigata, 940-2188, Japan*

Received 22 October 2004
Available online 10 December 2004

Abstract

The characteristics of the stress fields around a singular point on the stress singularity line of dissimilar materials in three-dimensional joints are investigated using BEM. Contour for the order of stress singularity around the point is mapped on Dundurs' parameters plane using eigen value analysis by FEM. The results in 3D joints are compared with those in 2D joints having the same cross section and material combination. The order of stress singularity around the singular point on the stress singularity line in 3D joints is almost identical with that in 2D joints in the singularity region. However, the zero boundary of singularity in 3D joints is slightly different from that in 2D joints. Furthermore, the multiple root of $p = 1$ exists in the eigen value analysis by FEM. Therefore, logarithmic singularity possibly occurs around the singular point on the stress singularity line. Then, the stress distributions around this point are expressed by the combination of the r^{λ} term and logarithmic singularity terms. Finally, the characteristics of the stress intensity factors of the r^{λ} term and logarithmic singularity terms around the singular points are investigated.

Keywords: Logarithmic singularity; Stress singularity; Three-dimensional joints; Dissimilar materials; BEM; Eigenequation; FEM

1. Introduction

In dissimilar materials, the stress singularity frequently occurs at a vertex of an interface due to a discontinuity of materials. It is, therefore, important to clarify the characteristic of the stress and displacement fields around a bonded edge. In the previous studies (Pageau and Biggers, 1995; Koguchi, 1997), the stress

* Corresponding author. Tel.: +81 901 933 2714; fax.: +81 258 47 9770.
E-mail addresses: monchai@stn.nagaokaut.ac.jp (M. Prukvilailert), koguchi@mech.nagaokaut.ac.jp (H. Koguchi).

0020-7683/$ - see front matter
doi:10.1016/j.ijsolstr.2004.10.027

singularity occurs not only at the vertex of the three-dimensional structure of dissimilar materials but also along the intersection of the interface with the free surface, and the cross line has been referred as a stress singularity line (see Fig. 1). The characteristics of the stress fields and their stress intensity factors around a point on the stress singularity line in dissimilar materials have been not made clear so far.

The two-dimensional asymptotic stress fields near an apex are expressed by a linear combination of $\sigma_{ij} \propto K_{ij} r^{p-1}$ or $\sigma_{ij} \propto L_{ij} r^{p-1} \ln r$ corresponding to roots p in $0 < \mathrm{Re}(p) < 1$, $\sigma_{ij} \propto L_{ij} \log r$ to a double roots at $p = 1$ as well as no singularity ones $\sigma_{ij} \propto K_{ij} r^{p-1}$ to roots p in $\mathrm{Re}(p) > 1$ (Bogy, 1970, 1971a,b; Bogy and Wang, 1971; Dempsey and Sinclair, 1979, 1981; Dempsey, 1995; Inoue et al., 1994, 1995, 1996), where r is a radial distance from an apex, and p is a root of an eigen equation. The constant values, K_{ij} and L_{ij}, for each solution indicate the stress intensity factors for the stress fields. Yang (1998a,b) and Gadi et al. (2000) examined the singular stress fields for the type of $\log r$ singularity that can be used to describe well for joints under thermal loading. As mentioned above, the characteristics of the stress fields in two-dimensional joints are represented in a form of r^{p-1} singularity or $\log r$ singularity depending on geometry of joints and loading conditions. However, there still are few investigations on the characteristics of the stress fields and the stress intensity factors around the vertex or the point on the stress singularity line of three-dimensional joints. The stress fields around the vertex of three-dimensional joints initially are defined only in a form of r^{p-1} singularity (Koguchi, 1997; Lee and Im, 2003). Afterwards, Koguchi et al. (2003) showed that the r^{p-1} singularity and logarithmic singularity possibly occur around the vertex of three-dimensional dissimilar materials joints, because the multiple root for $p = 1$ exists in the results of eigen value analysis based on FEM.

In this paper, the characteristics of the stress fields and the stress intensity factors around the singular point on the stress singularity line in three-dimensional dissimilar materials joints are investigated by a three-dimensional boundary element program. The order of stress singularity λ around this point is investigated using the three-dimensional eigen value analysis by FEM. We present the results for material combinations falling upon no singularity region, singularity region and at zero boundary of singularity on α_{2D}–β_{2D} Dundurs' parameters plane. The parameters, α_{2D} and β_{2D}, are defined as follows:

$$\alpha_{2D} = \frac{Km_2 - m_1}{Km_2 + m_1}$$
$$\beta_{2D} = \frac{K(m_2 - 2) - (m_1 - 2)}{Km_2 + m_1} \tag{1}$$

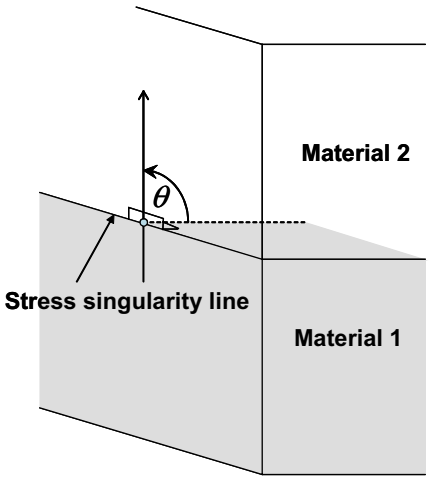

Fig. 1. Stress singularity line in a three-dimensional joint of dissimilar materials.

where

$$K = \frac{G_1}{G_2} \tag{2}$$

$$m_i = \begin{cases} 4(1-v_i) & \text{for plane strain} \\ \dfrac{4}{1+v_i} & \text{for plane stress} \end{cases} \quad (i = 1, 2) \tag{3}$$

in which G is shear modulus and v is Poisson's ratio. The subscript of these mechanical properties represents the region of materials; 1 refers to the lower region and 2 the upper region in Fig. 1.

2. Method and model for analysis

2.1. Eigen value analysis based on FEM

FEM formulation using an interpolation function of displacements, considering the stress singularity presented by Yamada and Okumura (1981) and Pageau and Biggers (1995) is used to analyze the order of stress singularity around the singular point on the stress singularity line. Fig. 2(a) shows the model for analysis. The singular point is at the origin in a spherical coordinate system. Taking the displacement at the origin as zero, the displacement in the i direction u_i at each node on the surface of FEM model near the singular point can be expressed as follow:

$$u_i(r, \theta, \phi) = r^p f_i(\theta, \phi) \tag{4}$$

where $p = \lambda + 1$. λ is the order of stress singularity. r, θ and ϕ are the spherical coordinates. Singular element with eight nodes using the serendipity quadratic interpolation function is employed for our analysis. Then, the eigen equation is derived by the principles of virtual work for deducing the root p,

$$(p^2[A] + p[B] + [C])\{u\} = 0 \tag{5}$$

There are many roots, p, obtained from solving the characteristic equation (Eq. (5)). Generally, the displacement fields around the singular point can be expressed as the following asymptotic series.

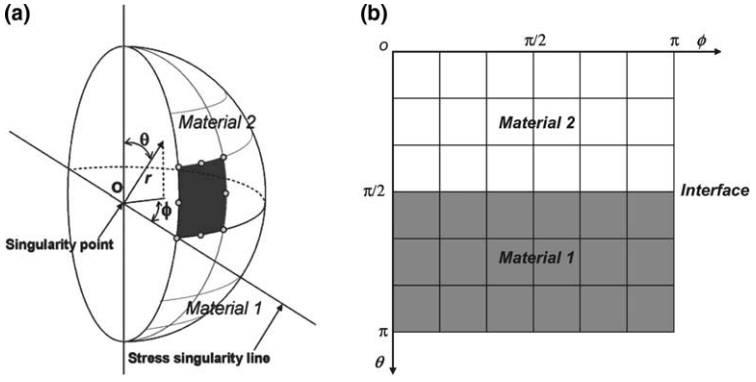

Fig. 2. Model of eigen analysis using FEM. (a) Model of a semispherical for eigen analysis using FEM. (b) Mesh division for eigen analysis using FEM.

$$u_i = \sum_{a=1}^{n} r^{p_a} f_{ia}(\theta, \phi, p_a) \tag{6}$$

where $f_{ia}(\theta, \phi, p_a)$ is the angular variation of displacement fields in the i direction. p_a is the ath root of an eigen equation. So, Eq. (5) can be factorized for n roots as

$$\prod_{a=1}^{n}(p - p_a) = 0 \tag{7}$$

when the multiple root of $p = p_1$ exist, Eq. (7) is rewritten as

$$(p - p_1)^m \prod_{a=2}^{n}(p - p_a) = 0 \tag{8}$$

where m is the number of the multiple root. In this case, the results of the displacement fields of Eq. (6) can not be obtained by calculating only one term of factor, but necessarily correspond with all multiple terms of factor. The answer of mth root can be obtained by calculating the derivative of order $(m-1)$th of the differential equation of the displacement fields with respect to p_1. Ordinarily, the differential equation of the displacement fields neglected the body force can be written by using the constitutive equations and strain–displacement relations as shown in the following expression.

$$N(u_i) = \left[\frac{\partial^2}{\partial x_j x_j} + \left(\frac{1}{1-2v}\right)\frac{\partial^2}{\partial x_i \partial x_j}\right] u_i = 0 \tag{9}$$

where $N(\,)$ represents a differential operator, which also satisfies the following expression as

$$\frac{\partial^j}{\partial p_1^j}[N(u_i)] = N\left[\left(\frac{\partial^j u_i}{\partial p_1^j}\right)\right] = 0 \tag{10}$$

If Eq. (4) satisfies Eq. (9) and the mth order term of factor exists, the displacements of the mth order term of factor can be written as follows:

$$\begin{aligned} u_{i,m} &= \frac{\partial^{m-1}}{\partial p_1^{m-1}}[r^{p_1} f_{i1}(\theta, \phi, p_1)] \\ &= r^{p_1}(\ln r)^{m-1} g_{i1}(\theta, \phi, p_1) + r^{p_1}(\ln r)^{m-2} g_{i2}(\theta, \phi, p_1) + \cdots + r^{p_1}(\ln r) g_{im-1}(\theta, \phi, p_1) \\ &\quad + r^{p_1} g_{im}(\theta, \phi, p_1) \end{aligned} \tag{11}$$

where $g_{ib}(b = 1, 2, \ldots, m)$ is the angular variation of the displacement fields in the i direction for logarithmic singularity terms as $p = p_1$. For example, the displacement component of the fifth order term of factor, $u_{i,5}$, is written in the same way.

$$N(u_i) = N\left[\left(\frac{\partial u_i}{\partial p_1}\right)\right] = N\left[\left(\frac{\partial^2 u_i}{\partial p_1^2}\right)\right] = N\left[\left(\frac{\partial^3 u_i}{\partial p_1^3}\right)\right] = N\left[\left(\frac{\partial^4 u_i}{\partial p_1^4}\right)\right] = 0 \tag{12}$$

$$\begin{aligned} u_{i,5} &= r^{p_1}(\ln r)^4 g_{i1}(\theta, \phi, p_1) + r^{p_1}(\ln r)^3 g_{i2}(\theta, \phi, p_1) + r^{p_1}(\ln r)^2 g_{i3}(\theta, \phi, p_1) + r^{p_1}(\ln r) g_{i4}(\theta, \phi, p_1) \\ &\quad + r^{p_1} g_{i5}(\theta, \phi, p_1) \end{aligned} \tag{13}$$

where if $p_1 = 1$, Eq. (13) becomes as follow

$$u_{i,5}(r, \theta, \phi) = r(\ln r)^4 g_{i1}(\theta, \phi) + r(\ln r)^3 g_{i2}(\theta, \phi) + r(\ln r)^2 g_{i3}(\theta, \phi) + r(\ln r) g_{i4}(\theta, \phi) + r g_{i5}(\theta, \phi) \tag{14}$$

Therefore, when five roots of $p_1 = 1$ exist, the displacement fields of the fifth order term of factor are composed of $r(\ln r)^4, r(\ln r)^3, r(\ln r)^2, r\ln r$ and r terms. Finally, the displacements fields around the singular point can be written by gathering the results for all terms of factor as

$$u_i(r,\theta,\phi) = rg_{i1}(\theta,\phi) + r(\ln r)g_{i2}(\theta,\phi) + r(\ln r)^2 g_{i3}(\theta,\phi) + r(\ln r)^3 g_{i4}(\theta,\phi) + r(\ln r)^4 g_{i5}(\theta,\phi) + \sum_{a=2} r^{p_a} f_{ia}(\theta,\phi,p_a) \tag{15}$$

Then, the expressions for the stress fields are obtained through the differentiation of displacements.

$$\sigma_{ij}(r,\theta,\phi) = L_{ij1}(\theta,\phi) + L_{ij2}(\theta,\phi)\ln r + L_{ij3}(\theta,\phi)(\ln r)^2 + L_{ij4}(\theta,\phi)(\ln r)^3 + L_{ij5}(\theta,\phi)(\ln r)^4 + \sum_{a=2} r^{\lambda_a} K_{ija}(\theta,\phi,p_a) \tag{16}$$

where L_{ijm} is the stress intensity factor of logarithmic singularity term ($m = 1,2,\ldots,5$), K_{ija} is that of r^{λ_a} term ($a = 2,3,\ldots,n$), and $\lambda_a = p_a - 1$. The subscripts i,j refer r,θ and ϕ in a spherical coordinate system. The domain for the eigen value analysis by FEM at the singular point on a stress singularity line is semi-spherical which the free surface and the interface plane are taken at $\theta = 0,\pi$ and $\theta = \pi/2$ respectively, and the mesh division used in this analysis is shown in Fig. 2(b). The square mesh size is employed as $\phi \times \theta = 18^\circ \times 18^\circ$ that the convergence rating and the time consumption for calculation are optimum.

2.2. Boundary element method

BEM is efficient for investigating the stress distribution in a three-dimensional joint structure, because it requires less memory than in the calculation of FEM for the large number of element. Furthermore, the accurate stress and displacement fields for any points in the joints with high stress sites can be obtained by preparing fine mesh data. The boundary integral equation in terms of the displacement vector, $\mathbf{u_j}$, and traction vector, $\mathbf{t_j}$, can be expressed as follows:

$$C_{ij}\mathbf{u_j}(P) = \int_A \{U_{ij}(P,Q)\mathbf{t_j}(Q) - T_{ij}(P,Q)\mathbf{u_j}(Q)\}\mathrm{d}s(Q) \tag{17}$$

where P and Q are points on the boundary. C_{ij} is a constant determined from the configuration of boundary. U_{ij} and T_{ij} are the fundamental solutions for displacement and surface traction, respectively. Here, Rongved's fundamental solution satisfying the boundary conditions at the interface is applied for our analysis.

A typical model employed in our calculation is shown in Fig. 3(a), where every free surface is a square in the same size, a side of which is 10 mm in length and the interface of joints is located at the middle of the upper and the lower surfaces. Parts indicated by shaded blocks as depicted in Fig. 3(a) are divided into a mesh utilizing the symmetry of joints configuration. The singular point $\mathbf{S}_i$ with a spherical coordinate system to estimate the stress distributions in the joint is taken on the stress singularity line as shown in Fig. 3(b). The stress fields around three singular points S_1, S_2 and S_3 on the stress singularity line are presented in order to investigate the stress distributions and the characteristics of the stress intensity factors in 3D joints. The distances from the singular points S_1, S_2 and S_3 to the vertex point are 0.0504, 0.0392 and 0.0292 mm, respectively. An example of mesh division for the joints is shown in Fig. 4, where the minimum length of an element near the singular point is 0.8 μm. The total number of elements is 1370 and the total number of nodes is 3067. The analyses are performed under the condition where a uniform constant tensile stress, $\sigma_{zz}(=P)$, is applied at the upper surface and the displacement in the z-direction only at the lower surface is fixed.

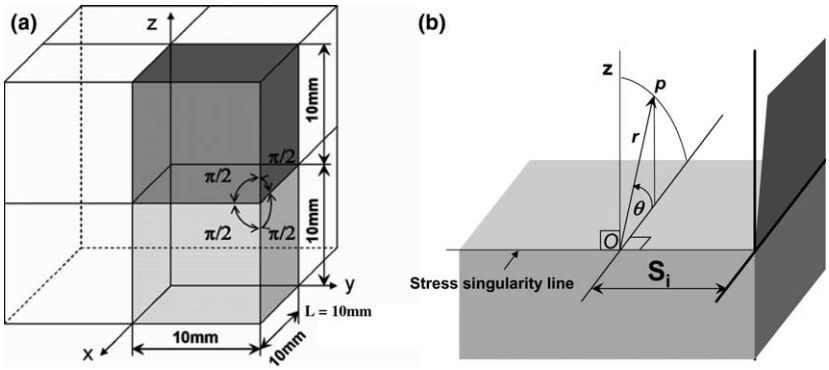

Fig. 3. A model for analysis in BEM and polar coordinate system around the singular point on the stress singularity line. (a) Model for analysis of joint. (b) Spherical coordinate system with the origin at the singular point S_i.

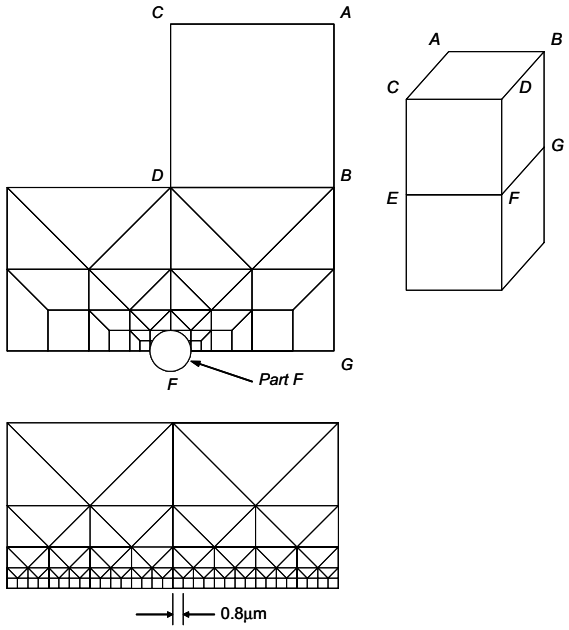

Fig. 4. Mesh division for model.

3. Results and discussion

3.1. The contour map of the order of stress singularity

Mechanical properties for material 1 in the analysis are fixed at 206.0 GPa for E_1 and 0.3 for v_1. E_2 and v_2 are determined by using Eq. (1)–(3), which can apply to any values of α_{2D} and β_{2D} in the plane strain condition. Then, the eigen value analysis by FEM is used to examine the order of stress singularity around the singular point on the stress singularity line for each material combination. The results in 3D joints are compared with those in 2D joints of the same cross section plane of 3D joints in the same material combination.

The order of stress singularity in 2D joints is also determined by using the eigen value analysis by FEM. Afterwards, the contour map of the order of stress singularity on Dundurs' composite plane is shown in Fig. 5 for the singular point on the stress singularity line in 3D joints and for the apex in 2D joints. The zero boundary of singularity in 2D joints is represented by two lines, $\alpha_{2D} = 0$ and $\beta_{2D} = \alpha_{2D}/2$. In this study, the point on the zero boundary of singularity in 3D joints is examined by varying the value of α_{2D} while holding β_{2D} at a fixed value until $-0.001 < \lambda_a < 0$ or $0.999 < p_a < 1.0$. Furthermore, the loci of the root of characteristic equations for the order of stress singularity, -0.05, -0.10, -0.15, and so on, are still investigated by varying the value of α_{2D} in the range $2\beta_{2D} \leqslant \alpha_{2D} \leqslant 1.0$ while holding β_{2D} at a fixed value. Then, the value of α_{2D} at $\lambda = -0.05$ to -0.35 is obtained by using the least-squares regression. In the singularity region, the contour of the order of stress singularity of 2D joints and 3D joints as well as the 2D analytical solution are almost identical to each other. From the previous study (Koguchi and Muramoto, 2000), it is noticed that the order of stress singularity around the singular point on the stress singularity line is less than that around the vertex of 3D joints. However, in the range of $\beta > 0.32$ and $\beta < 0.6$, the zero boundary of singularity in 3D joints does not seem to be the same line with that in 2D joints.

As the previous paper (Koguchi et al., 2003), it is found that the multiple root of $p = p_1 = 1$ exists in the result of the three-dimensional eigen value analysis by FEM, while two-dimensional eigen value analysis by FEM obtains only the single root of $p = 1$. Therefore, from the theory mentioned at the beginning of the section, the stress fields around the singular point on the stress singularity line in the 3D joints can be written possibly in a form of the combination of r^{λ} term and logarithmic singularity terms. From the three-dimensional FEM eigen value analysis, there are five roots of $p_1 = 1$ for logarithmic singularity terms and a root p_a for the r^{λ} term as shown in Tables 1–3. Therefore, the stress fields can be expressed as follows:

$$\sigma_{ij}(r,\theta,\phi) = L_{ij1}(\theta,\phi) + L_{ij2}(\theta,\phi)\ln r + L_{ij3}(\theta,\phi)(\ln r)^2 + L_{ij4}(\theta,\phi)(\ln r)^3 + L_{ij5}(\theta,\phi)(\ln r)^4 + r^{\lambda}K_{ija}(p_a,\theta,\phi) \tag{18}$$

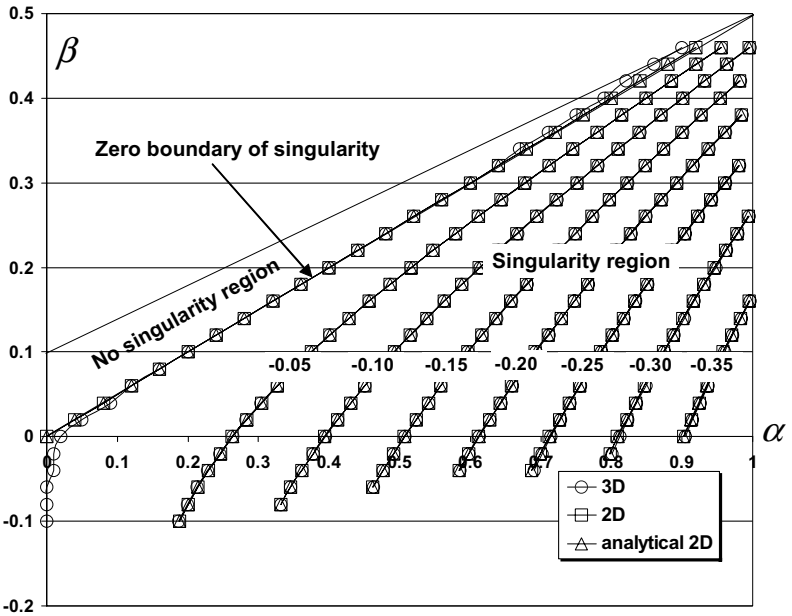

Fig. 5. The loci on the α_{2D}–β_{2D} of the order of stress singularity for two- and three-dimensional joints.

Table 1
Eigen values in $\alpha_{2D} = 0.1$ and $\beta_{2D} = 0.1$

	Real part of p	Imaginary part of p	$\lambda = \mathrm{Re}(p) - 1$
3D			
1	1.0081952	0.0000000	0.0081952
2	0.9991702	0.0000000	−0.0008298
3	0.9997747	0.0000000	−0.0002253
4	1.0001575	0.0000000	0.0001575
5	0.9999694	0.0000000	−0.0000306
6	1.0000497	0.0000000	0.0000497
2D			
1	1.0083351	0.0000000	0.0083351
2	1.0000000	0.0000000	0.0000000

Table 2
Eigen values in $\alpha_{2D} = 0.8$ and $\beta_{2D} = 0.2$

3D	Real part of p	Imaginary part of p	$\lambda = \mathrm{Re}(p) - 1$
1	0.7922460	0.0000000	−0.2077540
2	1.0011846	0.0000000	0.0011846
3	0.9990375	0.0000000	−0.0009625
4	1.0002454	0.0000000	0.0002454
5	1.0001365	0.0000000	0.0001365
6	1.0000081	0.0000000	0.0000081

Table 3
Eigen values in $\alpha_{2D} = 0.6$ and $\beta_{2D} = 0.3$

3D	Real part of p	Imaginary part of p	$\lambda = \mathrm{Re}(p) - 1$
1	0.9992602	0.0000000	−0.0007398
2	0.9996580	0.0000000	−0.0003420
3	1.0005570	0.0000000	0.0005570
4	1.0000740	0.0000000	0.0000740
5	1.0001653	0.0000000	0.0001653
6	1.0002720	0.0000000	0.0002720

3.2. Stress analysis of the singular points on the stress singularity line

In this section, the stress fields around the singular points S_1, S_2 and S_3 on the stress singularity line in 3D joints are investigated using BEM with Rongved's fundamental solution. The material combinations of a joint are determined so as to take the pairs of α_{2D} and β_{2D} locating in the no singularity region and the singularity region as well as at the zero boundary of singularity on Dundurs' composite plane. The stress fields are calculated along the r direction within $r/L \leqslant 10^{-2}$ in the range of $-60^\circ \leqslant \theta \leqslant 60^\circ$ on the plane that is perpendicular to a free surface and to an interface of dissimilar materials as shown in Fig. 3(b). The results in 3D joints are compared with those in the 2D joints FEM analyzed by MENTAT program in the same material combinations and boundary conditions. Then, we do the curve fitting of stress distribution along the r direction by using least-squares regression to obtain the stress intensity factor (L_{ijm}

$(m = 1,\ldots,5), K_{ija})$ of each term in Eq. (18). Afterwards, the characteristics of the stress intensity factors of r^{λ} term and logarithmic singularity terms are investigated.

3.2.1. Stress distribution in the no singularity region on Dundurs' composite plane

In this example, the material combination is at $\alpha_{2D} = 0.1$ and $\beta_{2D} = 0.1$ ($E_1 = 206\,\text{GPa}$, $\nu_1 = 0.3$, $E_2 = 181.3504\,\text{GPa}$, $\nu_2 = 0.14444$) where is in the no singularity region on Dundurs' composite plane. The stress distributions, σ_{ij}/P, along the r direction with various values of θ for the singular point S_1 are shown in Fig. 6(a)–(c) in log–log scale. The slope for each plot is always nearly and more than zeros. Therefore, it can be confirmed that there is no existing of r^{λ} singularity ($0 < \text{Re}(p_a) < 1$) around this point. Fig. 6(a) shows the log–log plots of $\sigma_{\theta\theta}/P$. For $\theta = -60°, 60°$, the plots are near to the free surface, so their magnitudes are very small. The stress level increases as approaches to the interface ($\theta = 0°$) of dissimilar materials. In case of $\sigma_{r\theta}/P$ in Fig. 6(b), the magnitude of the plot seems to become the highest one as θ approaches to 45°, and the stress level of σ_{rr}/P increases coming near the free surface as shown in Fig. 6(c). These distributions of the stress components are in accord with loading and boundary conditions.

The stress distributions of $\sigma_{\theta\theta}/P$ for three singular points S_1, S_2 and S_3 are plotted in semi-log scale in order to magnify the distributions as shown in Fig. 6(d). The profiles of the stress distributions are not

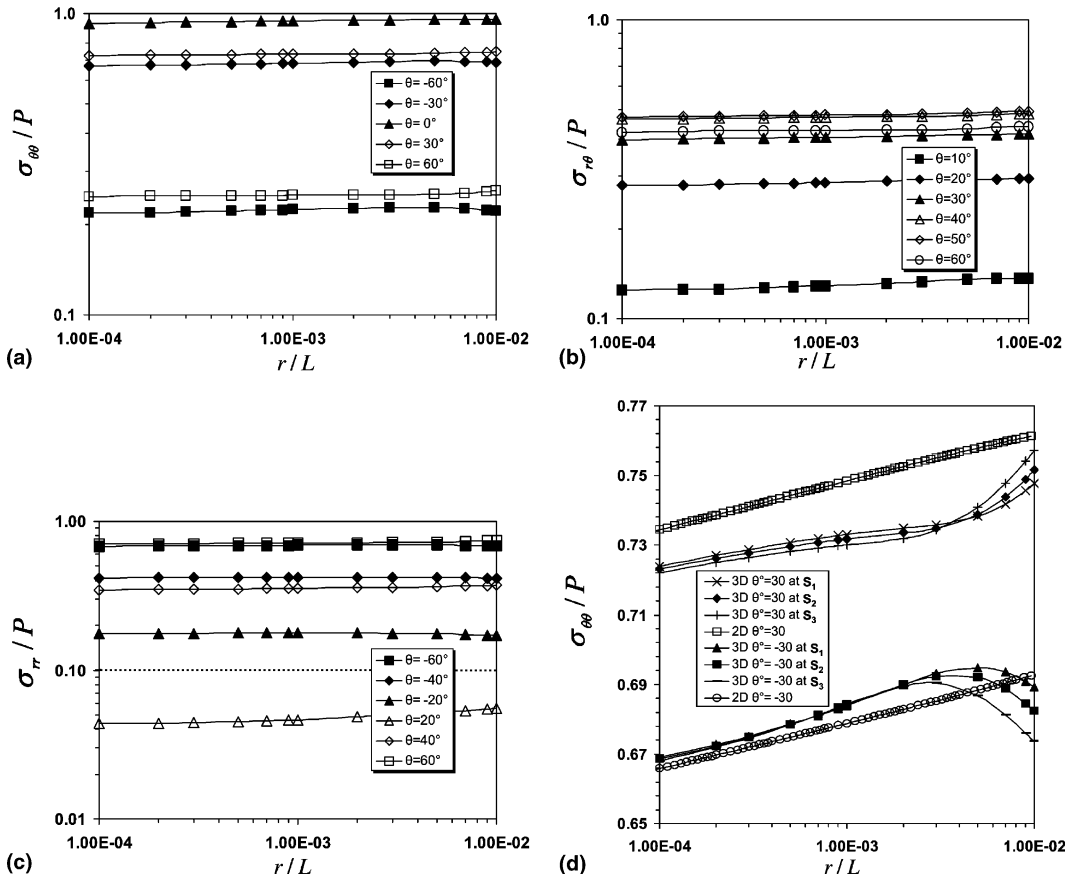

Fig. 6. The stress distributions around the singular point on the stress singularity line ($\alpha_{2D} = 0.1, \beta_{2D} = 0.1$). (a) A log–log plot of $\sigma_{\theta\theta}/P$ for the singular point S_1. (b) A log–log plot of $\sigma_{r\theta}/P$ for the singular point S_1. (c) A log–log plot of σ_{rr}/P for the singular point S_1. (d) A semi-log plot of $\sigma_{\theta\theta}/P$.

likely the simple line as in two-dimensional FEM analysis. However, the slopes of these lines are positive. It is noticed that the profiles of the stress distributions of $\sigma_{\theta\theta}/P$ for each singular point in 3D joints are different. From the calculation of two-dimensional FEM, λ is 0.008. It agrees well with three-dimensional FEM eigen value analysis that $\lambda > 0$ occurs and is equal to 0.00819 as shown in Table 1. In the previous section, five roots of $p_1 = 1$ occur in this region, and then the curve fitting of the stress distributions along the r direction is performed by defining $\lambda = 0.00819$ in Eq. (18). The stress intensity factors of r^{λ} term, K_{ija}/P, for the singular point S_1 are plotted against θ in Fig. 7(a). These profiles of $K_{\theta\theta a}/P$ and $K_{r\theta a}/P$ varying with θ are simple and continuous, while the profile of K_{rra}/P seems to be discontinuous at the interface. It is remarkable that the profiles of K_{ija}/P conform very well to the variation of the stress components level with θ in Fig. 6(a)–(c). The stress intensity factor $K_{\theta\theta a}/P$ decreases very little when the singular point comes toward the vertex point as shown in Fig. 7(b). Also, the profiles of $L_{\theta\theta m}/P$ for logarithmic singularity terms as the singular point is at S_1 are shown in Fig. 8(a). Their magnitudes at any values of θ are divided with the absolute value of $L_{\theta\theta m}/P$ at $\theta = -40°$ It is noticed that their profiles are closely similar to each other except their magnitudes that decrease rapidly with the increase of the power number of logarithmic term. For example, at $\theta = -40°$, the stress intensity factor of the constant term, $L_{\theta\theta 1}/P$, is -0.981 while the stress intensity factor of $\ln(r)^4$ term, $L_{\theta\theta 5}/P$, is only -0.000319. The characteristics of the stress intensity factor

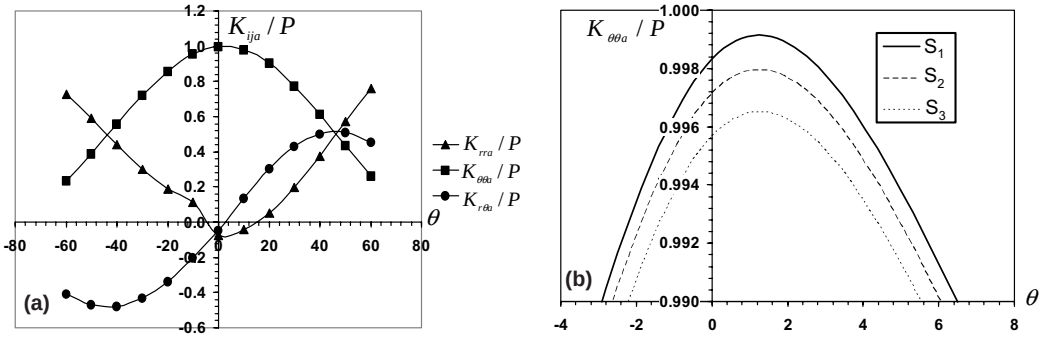

Fig. 7. The characteristics of the stress intensity factors of r^{λ} term ($\alpha_{2D} = 0.1, \beta_{2D} = 0.1$). (a) For the singularity point S_1. (b) The stress intensity factor $K_{\theta\theta a}/P$.

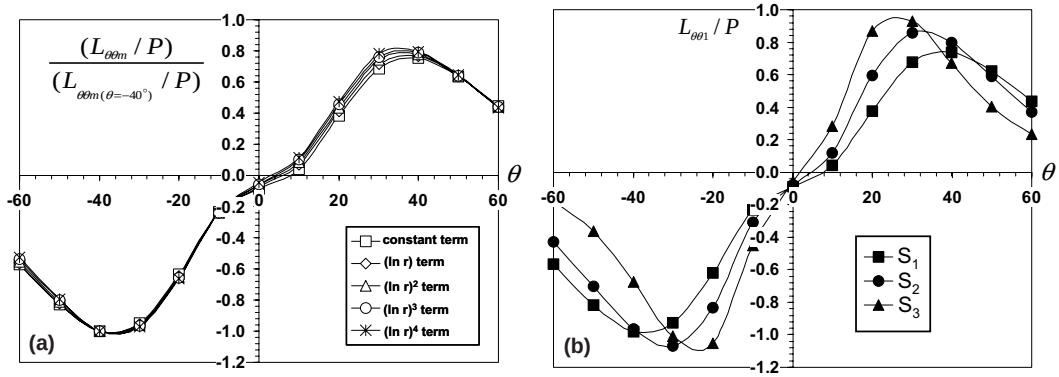

Fig. 8. The characteristics of the stress intensity factors of logarithmic singularity terms for $\sigma_{\theta\theta}/P$ ($\alpha_{2D} = 0.1, \beta_{2D} = 0.1$). (a) For the singularity point S_1. (b) The stress intensity factor $L_{\theta\theta 1}/P$.

of logarithmic singularity terms, $L_{\theta\theta m}/P$, are obviously different from that of r^{λ} term. In Fig. 8(b), the profile $L_{\theta\theta 1}/P$ also varies as the position of the singular point changes.

3.2.2. Stress distribution in the singularity region on Dundurs' composite plane

The stress distributions in the singularity region are investigated at the material combinations as $\alpha_{2D} = 0.8$ and $\beta_{2D} = 0.2$ ($E_1 = 206\,\text{GPa}$, $v_1 = 0.3$, $E_2 = 22.4170\,\text{GPa}$, $v_2 = 0.3293$) on Dundurs' composite plane. In Table 2, there are five roots of $p_1 = 1$ and a root $p_a = 0.792$. Fig. 9(a)–(c) show the log–log plots of the stress distributions, σ_{ij}/P, along the r direction for the singular point S_1. Slope of each line is almost

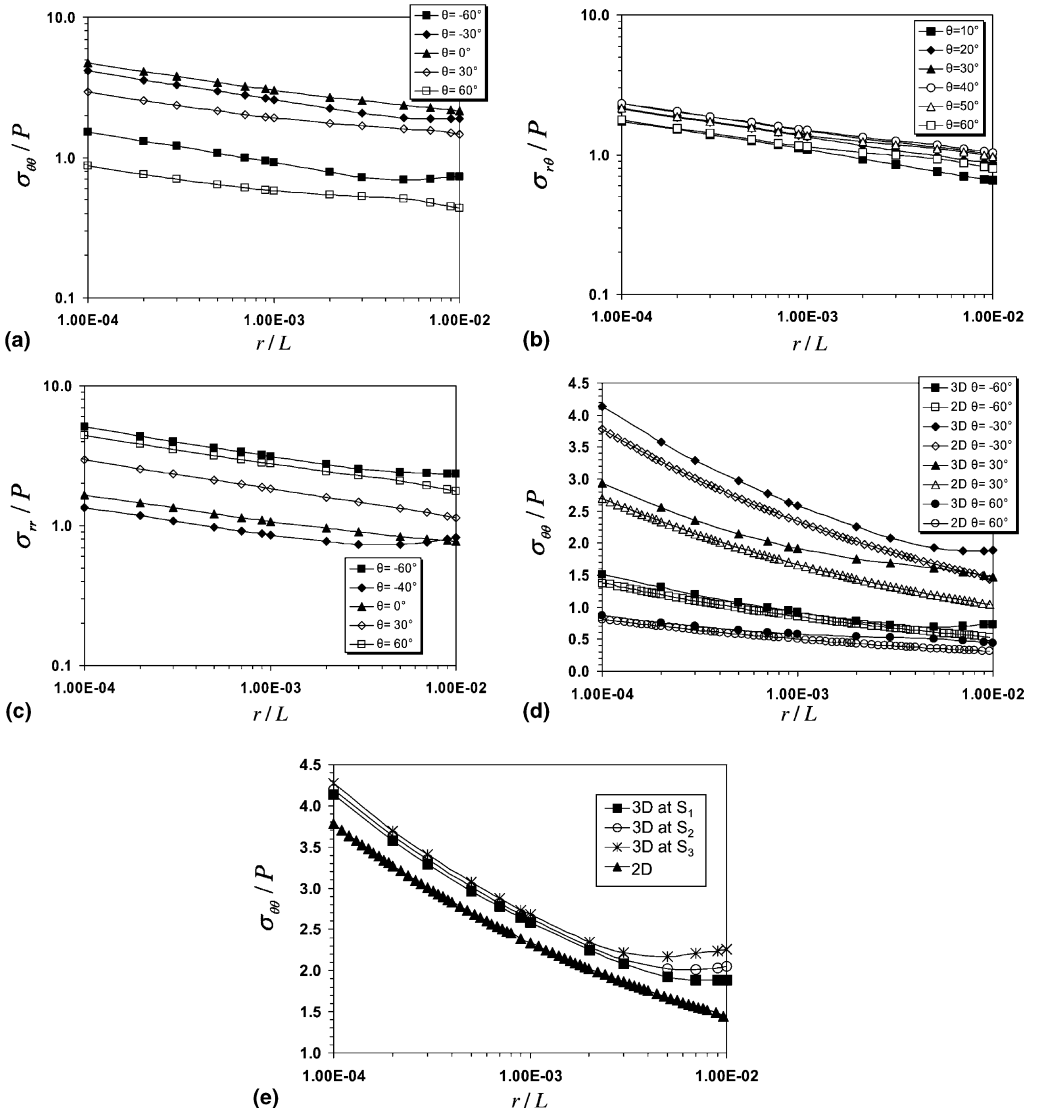

Fig. 9. The stress distributions around the singular point on the stress singularity line ($\alpha_{2D} = 0.8, \beta_{2D} = 0.2$). (a) A log–log plot of $\sigma_{\theta\theta}/P$ for the singular point S_1. (b) A log–log plot of $\sigma_{r\theta}/P$ for the singular point S_1. (c) A log–log plot of σ_{rr}/P for the singular point S_1. (d) A semi-log plot of $\sigma_{\theta\theta}/P$ for the singular point S_1. (e) A semi-log plot of $\sigma_{\theta\theta}/P$ at $\theta = -30°$.

the same value within $r/L \leqslant 10^{-2}$ and obviously less than zero. Therefore, the occurrence of the stress singularity in the form of the r^{λ} singularity is possible in this region. However, in the similar manner with the previous section, these plots also curve slightly as the distance from the singular point increases as shown explicitly in semi-log plots (see Fig. 9(d)). The plots of the stress distributions of $\sigma_{\theta\theta}/P$ in 3D joints are obviously different with those in 2D joint, and their magnitudes are larger. Furthermore, the magnitude of the stress distribution of $\sigma_{\theta\theta}/P$ also obviously increases with the decrease of the distance from the singular point to the vertex point as shown in Fig. 9(e). According to the results in Table 2, the least-squares regression is applied by setting $\lambda = p_a - 1 = -0.208$ in Eq. (18) for fitting the curves of the stress distributions. Then, the stress intensity factors of the r^{λ} singularity term, K_{ija}/P, for the singular points S_1, S_2 and S_3 in 3D joints and for the apex in 2D joints are plotted against θ in Fig. 10(a)–(c). Their profiles in 3D joints and 2D joints are almost similar with each other. It means that the characteristics of the stress distributions around the singular point on the stress singularity line in 3D joints surely consist of the stress distributions induced by the r^{λ} singularity term. The stress intensity factors of r^{λ} singularity term in 3D joints are obviously larger than those in 2D joints, and their magnitudes increase as the singular point comes closely to the vertex point. It is also noticed that the stress intensity factors of r^{λ} singularity term are larger and vary more rapidly in the region of material 1 ($E_1 = 206\,\text{GPa}$, $\nu_1 = 0.3$) than in that of material 2 ($E_2 = 22.4170\,\text{GPa}$, $\nu_2 = 0.3293$). The characteristic of K_{rra}/P in the singularity region differs obviously and reversely from that in the no singularity region. Furthermore, the profiles of $(L_{\theta\theta m}/P)/(L_{\theta\theta m\,\text{at}\,\theta=-40^{\circ}}/P)$ for the singularity point S_1 and the profiles of $L_{\theta\theta 1}/P$ for three singular points are shown in Fig. 11(a) and (b), respectively. These profiles are also reverse to the profiles of logarithmic singularity terms in the no singularity region.

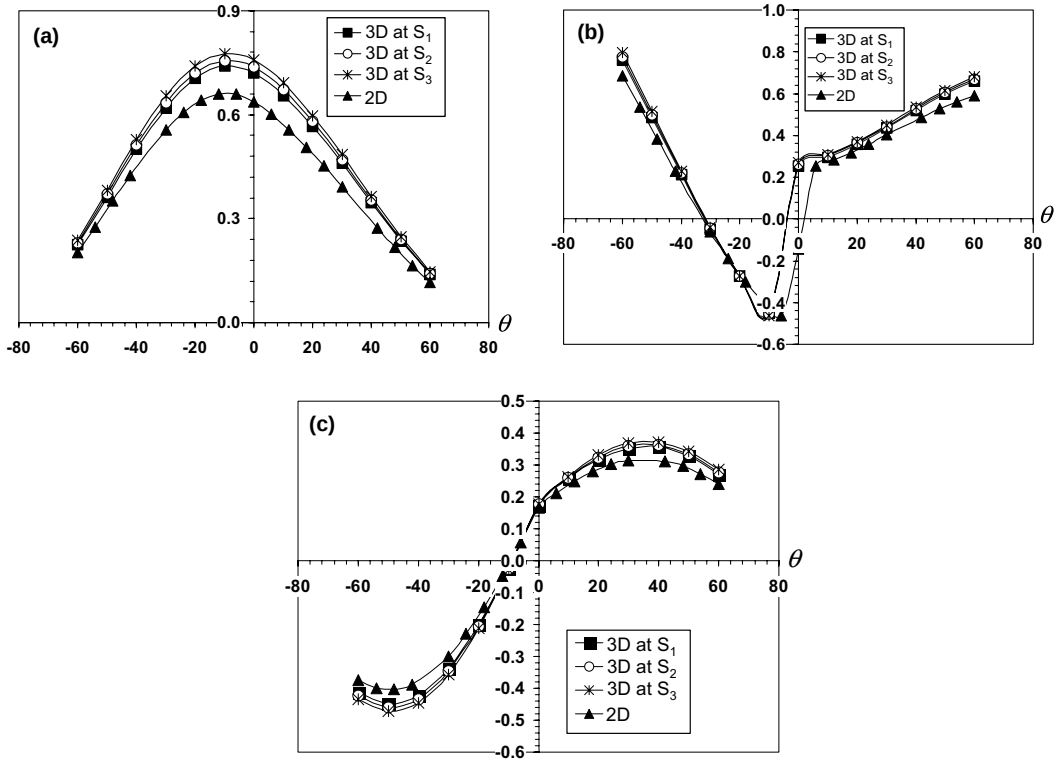

Fig. 10. The characteristics of the stress intensity factors of r^{λ} singularity term ($\alpha_{2D} = 0.8, \beta_{2D} = 0.2$). (a) $K_{\theta\theta a}/P$, (b) K_{rra}/P and (c) $K_{r\theta a}/P$.

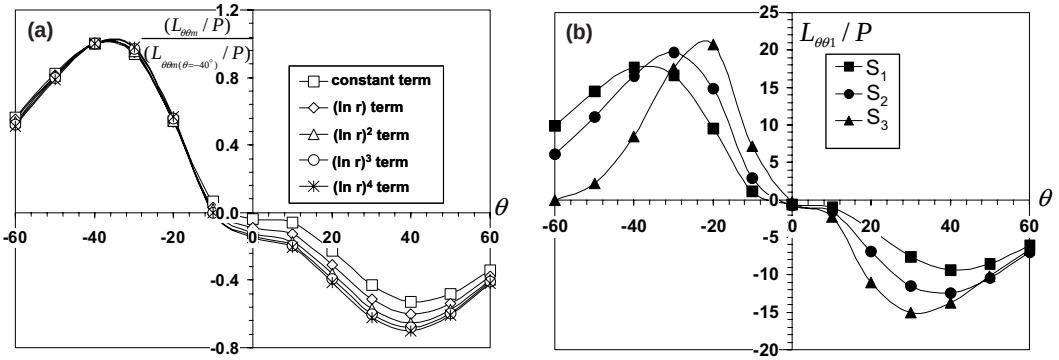

Fig. 11. The characteristics of the stress intensity factors of logarithmic singularity term for $\sigma_{\theta\theta}/P$ ($\alpha_{2D} = 0.8, \beta_{2D} = 0.2$). (a) For the singularity point S_1. (b) The stress intensity factor $L_{\theta\theta 1}/P$.

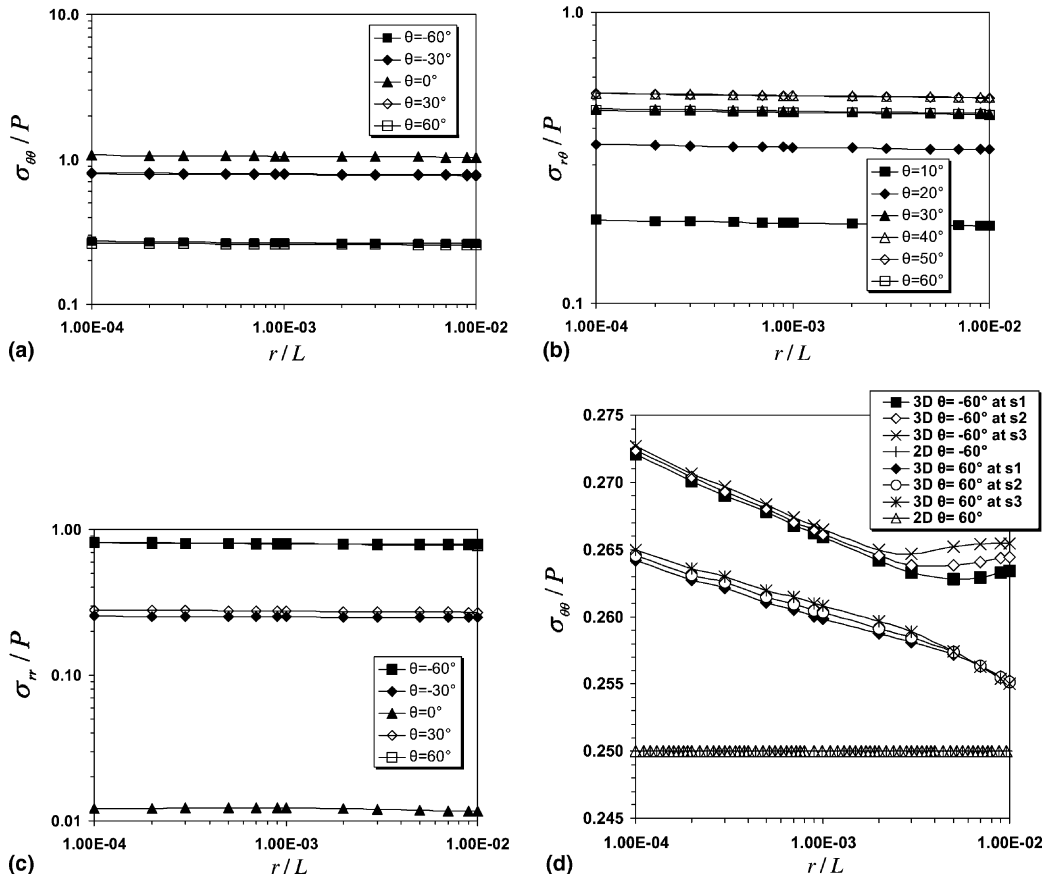

Fig. 12. The stress distributions around the singular point on the stress singularity line ($\alpha_{2D} = 0.6, \beta_{2D} = 0.3$). (a) A log–log plot of $\sigma_{\theta\theta}/P$ for the singularity point S_1. (b) A log–log plot of $\sigma_{r\theta}/P$ for the singularity point S_1. (c) A log–log plot of σ_{rr}/P for the singularity point S_1. (d) A semi-log plot of $\sigma_{\theta\theta}/P$.

Therefore, in the singularity region, the stress distributions also induce the r^{λ} singularity as well as the logarithmic singularity around the singular point.

3.2.3. Stress distribution at the zero boundary of singularity on Dundurs' composite plane

The material properties of dissimilar materials are determined to put Dundurs' composite parameter on the zero boundary of singularity in plane strain condition ($E_1 = 206\,\text{GPa}, v_1 = 0.3, E_2 = 56.0634$ GPa, $v_2 = 0.0968$) as $\alpha_{2D} = 0.6$ and $\beta_{2D} = 0.3$. According to the results in Table 3, there are five roots of $p_1 = 1$ and the very small r^{λ} singularity root $p_a = 0.99926$ ($\lambda = -0.00074$), so we also used Eq. (18) for fitting the curves of the stress distributions. The stress distributions, σ_{ij}/P, along the r direction for the singular point S_1 in Fig. 12(a)–(c) are shown that the slopes of log–log plots for a various θ are very small and seem to be zero. Furthermore, in semi-log plots as shown in Fig. 12(d), the plots of the stress distributions of $\sigma_{\theta\theta}/P$ for three singular points in 3D joints obviously curve, while the profiles of the plots are simple and flat in 2D joints.

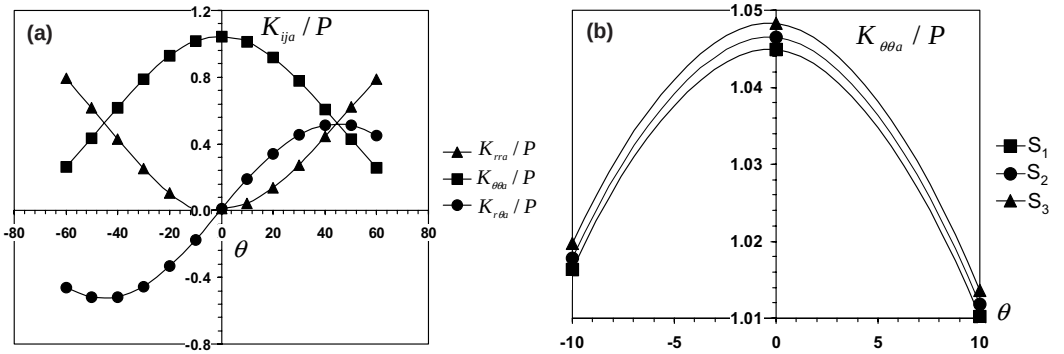

Fig. 13. The characteristics of the stress intensity factors for r^{λ} singularity term ($\alpha_{2D} = 0.6, \beta_{2D} = 0.3$). (a) For the singularity point S_1. (b) The stress intensity factor $K_{\theta\theta a}/P$.

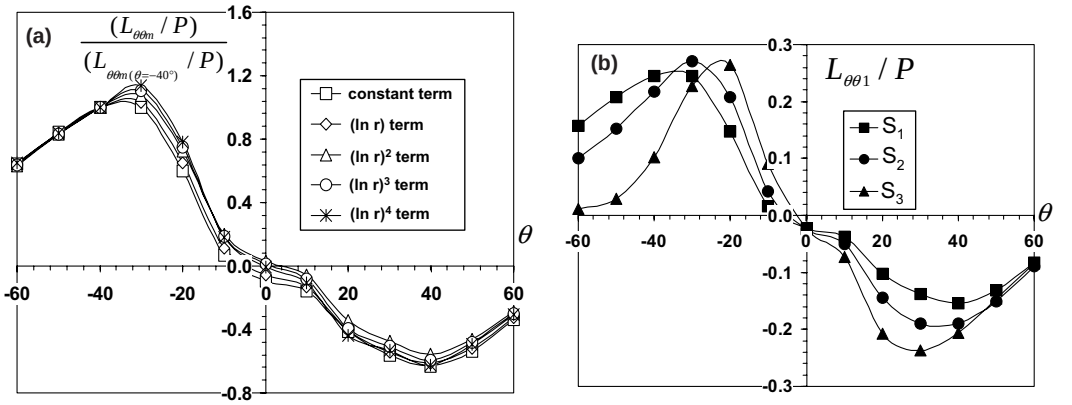

Fig. 14. The characteristics of the stress intensity factors of logarithmic singularity terms for $\sigma_{\theta\theta}/P(\alpha_{2D} = 0.6, \beta_{2D} = 0.3)$. (a) For the singularity point S_1. (b) The stress intensity factor $L_{\theta\theta 1}/P$.

The order of stress singularity obtained from an eigen value analysis by FEM is very small. Therefore, the logarithmic singularity mainly affects to the stress field much than the r^{λ} singularity at the zero boundary of singularity. Fig. 13(a) shows the characteristics of the stress intensity factors of the r^{λ} singularity term, K_{ija}/P. These plots are continuous and have almost the symmetrical shape with the interface, even if the mechanical properties of material 1 are quite different from those of material 2. Fig. 13(b) shows the profiles of the stress intensity factor $K_{\theta\theta a}/P$ for three singular points, and the characteristics of logarithmic singularity terms, $L_{\theta\theta m}/P$, for a various θ are shown in Fig. 14(a) and (b). These profiles conform to the profiles of the stress intensity factors for logarithmic singularity terms in the singularity region, but reverse to those profiles in the no singularity region.

4. Conclusion

We investigated the characteristics of stress singularity fields and their stress intensity factors at the points on the stress singularity line of dissimilar materials in three-dimensional joints. The order of stress singularity near these points was investigated using eigen value analysis by FEM. The contour map of the order of stress singularity was presented on a α_{2D}–β_{2D} plane in the plane strain condition. We found that the order of stress singularity around this singular point in three-dimensional joints was almost identical with that in two-dimensional joints. However, the bound vanishing the stress singularity in a three-dimensional stress state varied little compared to that in two-dimensional theory. Furthermore, the multiple root of $p = 1$ existed in the result of the three-dimensional FEM eigen value analysis. Therefore, the logarithmic singularity possibly occurred at the point on the stress singularity line in the three-dimensional joints. Then, the stress distributions and the characteristics of stress intensity factors for three singular points on the stress singularity line were investigated by BEM. The results showed that the stress fields at the points on the stress singularity line in three-dimensional joints were composed very well of the r^{λ} term and the logarithmic singularity terms.

References

Bogy, D.B., 1970. On the problem of edge-bonded elastic quarter-planes loaded at the boundary. Int. J. Solids Struct. 6, 1287–1313.

Bogy, D.B., 1971a. Two edge-bonded elastic wedges of different materials and wedge angles under surface tractions. J. Appl. Mech. 38, 377–386.

Bogy, D.B., 1971b. On the plane elastostatic problem of a loaded crack terminating at a material interface. J. Appl. Mech. 38, 911–918.

Bogy, D.B., Wang, K.C., 1971. Stress singularities at interface corners in bonded dissimilar isotropic elastic materials. Int. J. Solids Struct. 7, 993–1005.

Dempsey, J.P., 1995. Power-logarithmic stress singularities at bi-material corners and interface cracks. J. Adhes. Sci. Technol. 9, 253–265.

Dempsey, J.P., Sinclair, G.B., 1979. On the stress singularities in the plane elasticity of the composite wedge. J. Elasticity 9, 373–391.

Dempsey, J.P., Sinclair, G.B., 1981. On the singular behavior at the vertex of a bi-material wedge. J. Elasticity 11, 317–330.

Gadi, K.S., Joseph, P.F., Zhang, N., Kaya, A.C., 2000. Thermally induced logarithmic stress singularities in a composite wedge and other anomalies. Eng. Fract. Mech. 65, 645–664.

Inoue, T., Koguchi, H., 1996. Influence of the intermediate material on the order of the stress singularity in three-phase bonded structure. Int. J. Solids Struct. 33, 399–417.

Inoue, T., Koguchi, H., Yada, T., 1994. Analysis near the apex in three-phase bonded material with arbitrary wedge angles under normal surface loading on the surface (1st report, stress distribution in the stress fields with singularity of type $r^{-\lambda}$ and $\log r$). Trans. Jpn. Soc. Mech. Eng. (A) 61-581, 73–79 (in Japanese).

Inoue, T., Koguchi, H., Yada, T., 1995. Solution of thermal stresses near apex in dissimilar materials by thermoelastic theory. Trans. Jpn. Soc. Mech. Eng. (A) 61-581, 73–79 (in Japanese).

Koguchi, H., 1997. Stress singularity analysis in three-dimensional bonded structure. Int. J. Solids Struct. 34, 461–480.

Koguchi, H., Muramoto, T., 2000. The order of stress singularity near the vertex in three-dimensional joints. Int. J. Solids Struct. 37, 4737–4762.

Koguchi, H., Yamaguchi, M., Minaki, K., Monchai, P., 2003. Analysis of stress singularity fields in three-dimensional joints by three-dimensional boundary element method using fundamental solution for two-phase transversely isotropic materials. Trans. Jpn. Soc. Mech. Eng. (A) 69-679, 585–593 (in Japanese).

Lee, Y., Im, S., 2003. On the computation of the near-tip stress intensities for three-dimensional wedges via two-state *M*-integral. J. Mech. Phys. Solids 51, 825–850.

Pageau, S.S., Biggers Jr., S.B., 1995. Finite element evaluation of free-edge singular stress fields in anisotropic materials. Int. J. Numer. Methods Eng. 38, 2225–2239.

Yamada, Y., Okumura, H., 1981. Analysis of local stress in composite materials by the 3-D finite element. In: Proc. of the Japan–US Conference, Tokyo p. 55–64.

Yang, Y.Y., 1998a. Stress analysis in a joint with a functionally graded material under a thermal loading by using the Mellin transform method. Int. J. Solids Struct. 35, 1261–1287.

Yang, Y.Y., 1998b. Asymptotic description of the logarithmic singular stress field and its application. Int. J. Solids Struct. 35, 3917–3933.